ARTICLE OPEN

Check for updates

Regulation of Src tumor activity by its N-terminal intrinsically disordered region

Emilie Aponte[1,2,7], Marie Lafitte[1,2,7], Audrey Sirvent[1,2], Valérie Simon[1,2], Maud Barbery[1,2], Elise Fourgous[1,2], Yvan Boublik[1,2], Mariano Maffei[3,4], Florence Armand[5], Romain Hamelin[5], Julie Pannequin[6], Philippe Fort[1], Miquel Pons[3,7]✉ and Serge Roche[1,2,6,7]✉

The membrane-anchored Src tyrosine kinase is involved in numerous pathways and its deregulation is involved in human cancer. Our knowledge on Src regulation relies on crystallography, which revealed intramolecular interactions to control active Src conformations. However, Src contains a N-terminal intrinsically disordered unique domain (UD) whose function remains unclear. Using NMR, we reported that UD forms an intramolecular fuzzy complex involving a conserved region with lipid-binding capacity named Unique Lipid-Binding Region (ULBR), which could modulate Src membrane anchoring. Here we show that the ULBR is essential for Src's oncogenic capacity. ULBR inactive mutations inhibited Src transforming activity in NIH3T3 cells and in human colon cancer cells. It also reduced Src-induced tumor development in nude mice. An intact ULBR was required for MAPK signaling without affecting Src kinase activity nor sub-cellular localization. Phospho-proteomic analyses revealed that, while not impacting on the global tyrosine phospho-proteome in colon cancer cells, this region modulates phosphorylation of specific membrane-localized tyrosine kinases needed for Src oncogenic signaling, including EPHA2 and Fyn. Collectively, this study reveals an important role of this intrinsically disordered region in malignant cell transformation and suggests a novel layer of Src regulation by this unique region via membrane substrate phosphorylation.

Oncogene (2022) 41:960–970; https://doi.org/10.1038/s41388-021-02092-x

INTRODUCTION

Src, originally identified as an oncogene, is a membrane-anchored tyrosine kinase, which mediates signaling induced by a wide range of cell surface receptors, leading to cell growth and adhesion [1]. Src deregulation is associated with cancer development, although the underlying mechanisms are not fully understood [2, 3]. Src shares with the other Src Family Kinases (SFKs) a common modular structure formed by the membrane-anchoring SH4 region followed by an intrinsically disordered region (IDR) named unique domain (UD), and the SH3, SH2, and kinase domains [2]. Our knowledge of Src regulation relies on crystallographic data that revealed SH2 and SH3-dependent intramolecular interactions that control Src catalytic activity [4]. However, the functions of the SH4-UD module have often been disregarded because of X-ray invisibility. UD is the mostly divergent part of SFK proteins, which supported the idea of a unique function among SFKs [5, 6]. However, early studies reported that the whole UD deletion does not affect Src oncogenic activity [7], which suggests that this region may not play an important role in Src signaling. While considerable insight into Src regulation has been provided since the discovery of the Src oncogene, the functional role of its unstructured region remains unclear.

IDRs are highly prevalent in proteins regulating essential cell processes, such as transcription or signaling that are implicated in human diseases [8]. The integration of multiple weak interactions is crucial for the increasingly recognized role of IDRs in the formation of membrane-less organelles, through liquid-liquid phase separation [8]. Multiple, rapidly exchanging weak contacts are also at the basis of the formation of the so called "fuzzy complexes" by IDRs, in which the IDR remains disordered, but the complex is stabilized by multiple transient contacts [5, 9]. Intramolecular fuzzy complexes involve a similar fuzzy interaction between an IDR and a globular domain in the same protein to form a relatively compact structure [5, 9]. Intramolecular fuzzy complexes may regulate the communication between the disordered and globular regions of a signaling protein and sense the environment (e.g., membrane lipids) that will influence the activity of folded domains, such as kinase activity or the binding capacity of SH2 and SH3 domains [5, 9]. Thus, IDRs provide a unique mechanism of protein regulation by the local environment. In line with this, recent molecular studies uncovered key features of such a new Src-UD regulatory mechanism [10–13]. Specifically, Src-UD forms an intramolecular fuzzy complex, where its conformational freedom is restricted by multiple contacts with

[1]CRBM, CNRS, Univ. Montpellier, F-34000 Montpellier, France. [2]Equipe labellisée Ligue Contre le Cancer, CRBM, CNRS, Univ. Montpellier, F-34000 Montpellier, France. [3]Biomolecular NMR laboratory, Department of Inorganic and Organic Chemistry, University of Barcelona, Baldiri Reixac 10-12, 08028 Barcelona, Spain. [4]Evvivax srl—Via di Castel Romano, 100 - 00128 Rome, Italy. [5]Proteomics Core Facility, School of Life Sciences, École Polytechnique Fédérale de Lausanne (EPFL), 1015 Lausanne, Switzerland. [6]IGF, CNRS, Univ. Montpellier, F-34000 Montpellier, France. [7]These authors contributed equally: Emilie Aponte, Marie Lafitte, Miquel Pons, Serge Roche. ✉email: mpons@ub.edu; serge.roche@crbm.cnrs.fr

Received: 22 April 2021 Revised: 14 October 2021 Accepted: 21 October 2021
Published online: 9 January 2022

the globular SH3 domain [11]. Although their primary sequences are divergent, UD fuzzy complexes are present in other SFKs, suggesting that this IDR defines a central regulatory mechanism in SFKs [14, 15]. Our molecular studies on Src identified a conserved region that contributes to the interaction of the UD with the RT and nSrc loops of the SH3 domain [10, 11]. This region displays affinity with phospholipids and was named Unique Lipid-Binding Region (ULBR) [10]. Further NMR studies showed that ULBR participates in the interaction between the N-terminal myristoyl group and the SH3 domain. In the presence of membrane lipids, this region contributes to the modulation of Src membrane anchoring by placing the SH3 domain close to the membrane surface and restricting its orientation [13]. These in vitro results suggest that ULBR could also be involved in Src substrate selection and signaling by modulating the Src topology at the inner face of the membrane. Here we start addressing the oncogenic relevance of the Src UD by focusing on ULBR.

RESULTS

Evolutionary conservation of ULBR in SFK-UD

Although Src-UD is thought to be evolutionary conserved, we noticed a strong sequence divergence between mammalian and invertebrates SFKs. To clarify this point, we readdressed SFK sequence conservation by comparing the selective constraints exerted along SFK sequences. We computed ω, the ratio of nonsynonymous (dN) to silent (dS) mutations from a multiple alignment of Src, Yes and Fyn coding sequences of seven primate species, covering 74 million years of evolution. In such framework, neutral selection is associated with an ω-value close to 1, while values <1 or >1 indicate purifying and diversifying selection, respectively. As shown in Fig. 1a, all domains produced ω-values <1. However, UD ω-values indicated variable selection levels depending on SFK members. Notably, the heaviest selection was exerted on Fyn UD (ω = 0.0001), while the selection exerted on Src UD was moderate (ω = 0.126) and even lighter for Yes (ω = 0.363).

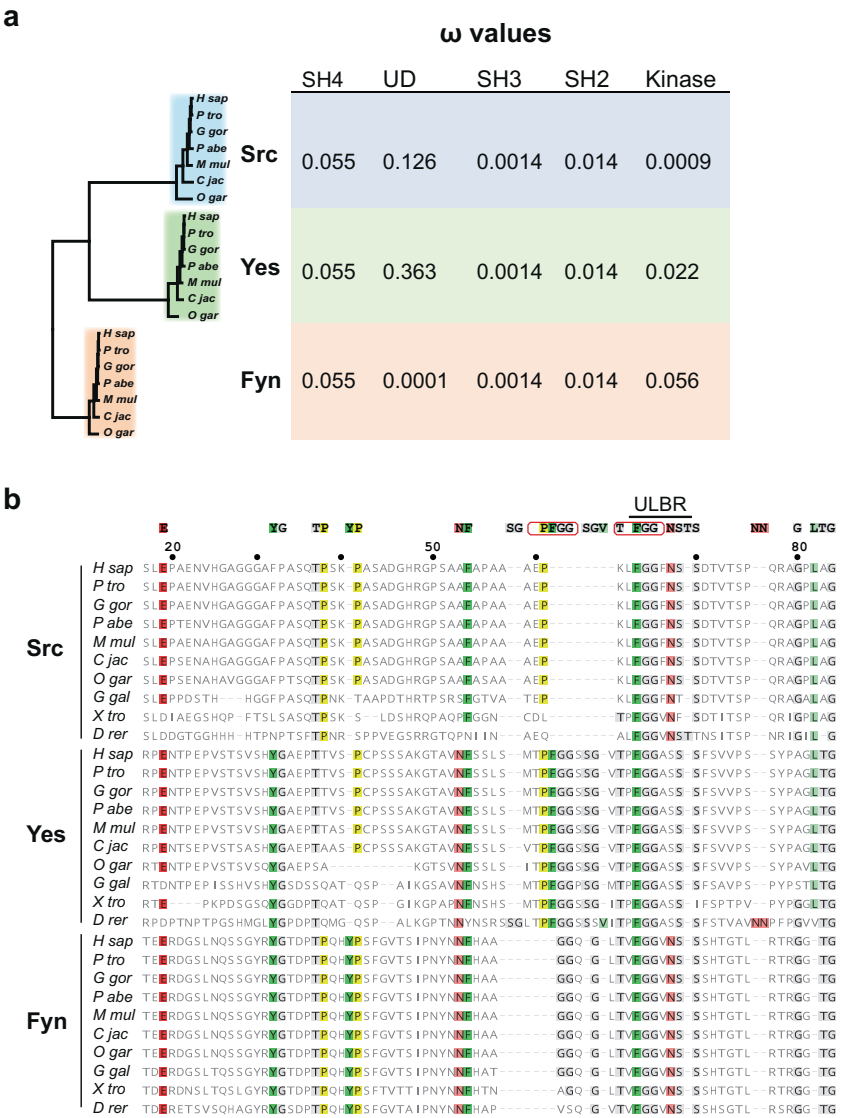

Fig. 1 Evolutionary conservation of the UD in SFKs. a Analysis of dN/dS ratios (ω) of the SH4, UD, SH3, SH2 and kinase domains in primate SFKs. Nucleic sequences coding the different domains were aligned based on translation and processed by codeml to estimated ω-values. The phylogenetic tree on the left was generated by PhyML analysis of a multiple alignment of full-length SFK sequences. **b** Multiple alignment of UD sequences of primate SFKs. Sequences were aligned with MAFFT. The most conserved residues are indicated above the alignment. The strictly conserved FGG of the ULBR is framed. Numbering corresponds to human c-Src sequence. H sap Homo sapiens, P tro Pan troglodytes, G gor Gorilla gorilla, P abe Pongo abelii, M mul Macaca mulatta, C jac Callithrix jacchus, O gar Otolemur garnettii, G gal Gallus gallus, X tro Xenopus tropicalis, D rer Danio rerio.

This indicates that UD sequences are not under neutral selection and supports the notion that these sequences play essential roles in SFKs functions. Consistent with this idea, a comparative sequence analysis of SFK-UD IDR sequences from 10 vertebrate species revealed that residues 64-Phe-Gly-Gly-66 (human Src numbering) are highly conserved across species and also across the three functional related Src, Fyn and Yes. They are part of the conserved Src ULBR (residues 60–67) highlighting an important function for this small region (Fig. 1b).

ULBR inactivation affects Src oncogenic activity

We next explored the functional role of Src-ULBR on cell transformation. For this, we performed a mutagenesis analysis guided from our previous NMR data to specifically inactivate ULBR molecular properties [10, 11, 13, 14, 16] (Fig. 2a). First, ULBR was inactivated by replacement of residues 63–65 (Leu-Phe-Gly) by three alanines (named Src3A), which affects its binding to phospholipids and SH3, and its modulatory function on Src membrane anchoring [10, 11, 13]. Second, since these ULBR properties can be inhibited in a similar fashion by phosphorylation of surrounding Ser69 and Ser75 in vitro [10, 17], we also inactivated ULBR by replacement of Ser69 or Ser75 by the phospho-mimicking glutamic acid (i.e., SrcS69E and SrcS75E) (Fig. 2a). These ULBR mutations were incorporated in the oncogenic SrcY530F mutant, in which the pTyr530-SH2 interaction is destabilized, thereby inducing an active and open Src conformation [4]. Transforming activity was then assessed upon retroviral transduction in immortalized mouse embryonic fibroblasts NIH3T3 (Fig. 2b–d). SrcY530F protein levels were reduced compared to regulated Src (Fig. 2b), which was previously attributed to an autoregulatory mechanism mediated by the substrate and E3 ligase Cbl [18]. Despite this and unlike wild-type Src, oncogenic SrcY530F expression induced anchorage-independent growth as measured by the number of colonies in soft agar. Interestingly, ULBR inactive mutations strongly reduced this transforming effect, suggesting that an intact ULBR is required for oncogenic Src activity (Fig. 2c). The invasive properties of NIH3T3 cells were also reduced, as assayed in Boyden chambers coated with matrigel (Fig. 2d). However, other transformation related properties induced by SrcY530F, such as dissolution of F-actin bundles causing actin cytoskeletal rearrangement (Supplementary Fig. S1c) [19], were retained in ULBR mutants. This indicates that ULBR selectively regulates some of Src transforming activities.

We next addressed the importance of ULBR in Src transforming activity in human cancer. In spite of the fact that *SRC* somatic mutations are rarely detected in human malignancies, aberrant Src activity, resulting from pathological deregulation, is a bad prognosis maker in epithelial tumors and has important roles during tumor development/progression [2, 3]. In colon cancer cells, regulation of Src signaling is highly perturbed due to defects in the regulation of its catalytic activity due to CSK inactivation [20], which mediates Src-Tyr530 phosphorylation [4]. Defects in the regulation of Src substrates degradation, due to inactivation of the inhibitory signaling protein SLAP in these tumor cells also participates in Src oncogenic signaling [21]. As a result, ectopic expression of wild type Src in SW620 colon cancer cells, which originate from a lymph node metastasis and express low levels of endogenous Src, strongly increases their growth and invasive and abilities [22, 23] (Fig. 2e–g). Expression of ULBR mutated Src produced similar results as in fibroblasts, i.e., a strong diminution of both anchorage-independent cell growth and cell invasion (Fig. 2f, g). Importantly, subcutaneous injection of these tumor cells in *nude* mice produced similar results. In this experimental in vivo cancer model, Src expression enhanced tumor development by 8-fold as compared to control cells, while this effect was reduced by 60% upon Src3A mutant expression (Fig. 3a, b). Immuno-histochemical analysis of tumor sections showed a significant reduction in colon cancer cell proliferation in Src3A samples (Fig. 3c). In contrast to wild-type Src, Src3A significantly increased tumor cells apoptosis (Fig. 3d). Src also induced a substantial increase in tumor angiogenesis, important for tumor progression. While the overall length of tumor vessels was not significantly modified by ULBR inactivation, we noted a significant diminution of tumor vessels with a length <30 µm in Src3A expressing tumors, suggesting an implication of this region during tumor angiogenesis (Fig. 3e).

ULBR inactivation affects Src oncogenic signaling

We next investigated the mechanisms involved in Src-ULBR function. Oncogenic SrcY530F induced a large increase of protein tyrosine phosphorylation in NIH3T3 cells, which was substantially reduced upon ULBR inactivation (Supplementary Figs. S1a and S2a). ULBR mutants also showed a reduction in SFKs activity, as measured by the level of their conserved tyrosine phosphorylation localized in the activation loop (i.e., pTyr419 in Src) (Supplementary Figs. S1a and S2a), with respect to the one observed in SrcY530F. This suggests that, in the context of oncogenic SrcY530F in NIH3T3 cells, ULBR regulates both substrate phosphorylation and SFK activity. Similar results were observed in HEK293T cells, in which transiently expressed Src resulted in high level of Src activity due to high ectopic kinase expression and low endogenous CSK levels [24]. In this context, Src induced a large increase in protein tyrosine phosphorylation, which was dependent upon a functional ULBR (Fig. 4a and Supplementary Fig. S2b). Src3A also showed a 20% reduction in SFK activity as compared to wild-type Src (Fig. 4a and Supplementary Fig. S2b). We next searched for a similar mechanism operating in human cancer. Consistent with a robust transforming activity, retroviral transduction of wild-type Src in SW620 cells increased protein tyrosine phosphorylation. As in HEK293T cells, 3A ULBR mutation caused a reduction in substrate phosphorylation but a reduction in active Src level was not evident (Fig. 4b and Supplementary Fig. S2c). The regulatory role of ULBR on Src signaling was next confirmed on MAPK activity, an important downstream effector of Src transforming activity in epithelial cells [25]. ULBR mutations reduced Src-induced p42/44 MAPKs activation both in HEK293T cells and SW620 tumor cells (Fig. 4a, b, Supplementary Fig. S2b & c). A similar effect of ULBR inactivation was observed on oncogenic Src signaling in NIH3T3 cells. Src has been shown to induce fibroblasts cell transformation by a p38 MAPK and Stat3-dependent signaling mechanism [26, 27]. Accordingly, SrcY530F transforming activity was accompanied by an increase in pTyr507-Stat3 and p38 signaling, which was reduced upon ULBR inactivation (Supplementary Figs. S1b and S2a).

We next searched for the molecular mechanisms implicated in ULBR-dependent Src substrates phosphorylation. The Src-UD has been suggested to participate in protein dimerization, enabling kinase activation [12, 28]. We tested the possible ULBR contribution to this molecular process. For this, Src constructs tagged with a hemagglutinin (HA) or a FLAG sequence at the C terminus were co-transfected in HEK293T cells, and Src self-association was assessed by co-immunoprecipitation. Src dimerization was not detected, unless when using stringent lysis conditions (i.e., RIPA buffer) [20, 29]. This suggests that dimerization may occur in cholesterol-enriched membrane domains, consistent with lipid-binding-induced dimerization/oligomerization observed in SH4 myristoylated Src derivatives [28, 30]. Using these conditions, we did not detect any effect of ULBR inactivation on Src self-association, indicating that this conserved region may not be involved in kinase dimerization (Fig. 4c). We next evaluated the role of ULBR on Src subcellular localization. For this, Src constructs (wild-type or ULBR mutants) were generated with either a GFP or mCherry tag at the C terminus together with a spacer (GluX3) for molecular constraint limitation between GFP (or mCherry) and Src (Supplementary Fig. S3a). Wild-type Src fused to mCherry was co-expressed with Src-ULBR mutants fused to GFP in HEK293T cells

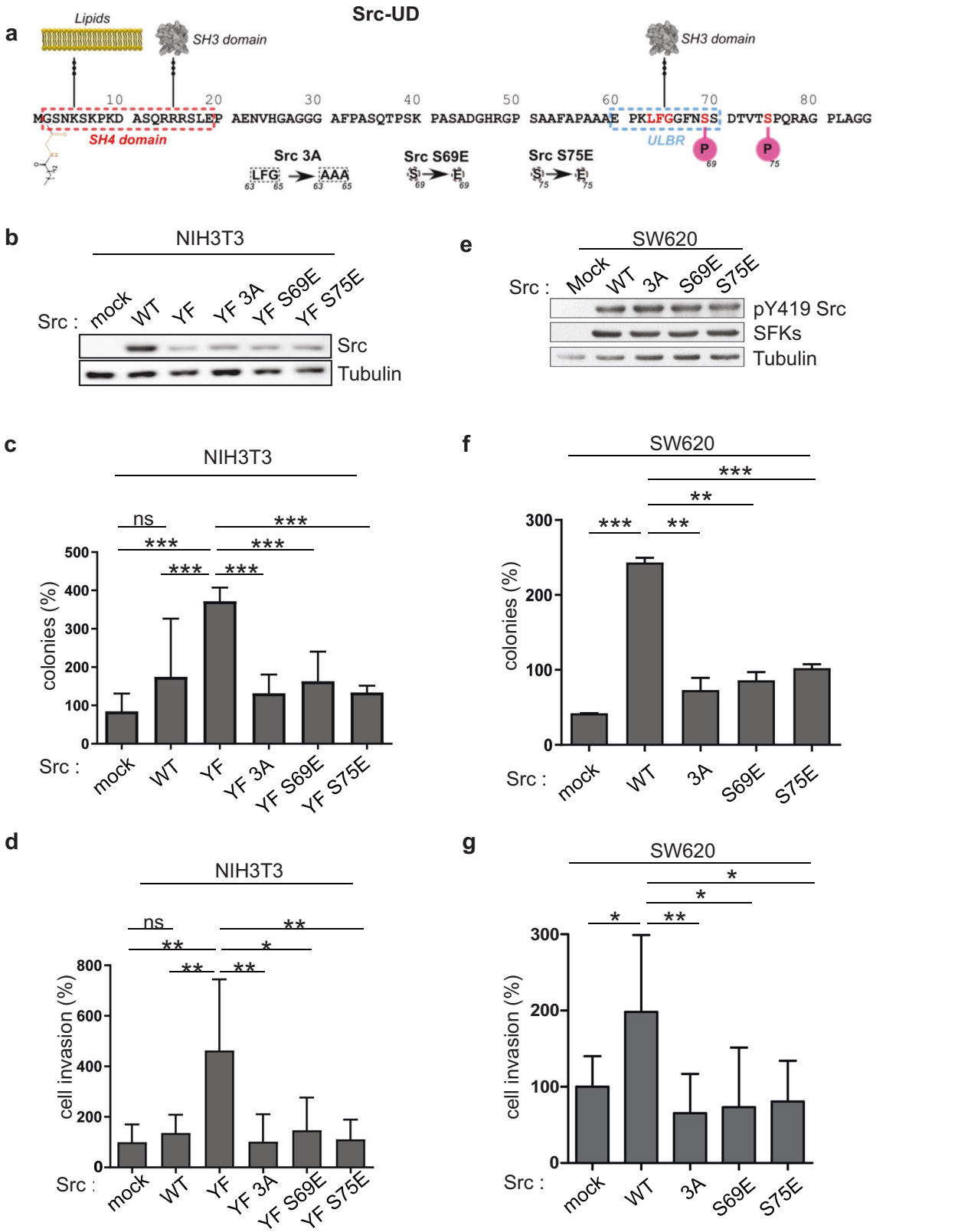

Fig. 2 ULBR inactivation affects Src oncogenic activity. a Strategy of ULBR inactivation. Molecular properties of Src-ULBR including amino acids involved in this process are highlighted. **b** the level of Src expression in NIH3T3 cells transduced with indicated Src constructs. Anchorage-independent cell growth (**c**) and invasion (**d**) of indicated Src-transformed NIH3T3 cells. **e** The level of Src expression and activity in SW620 colon cancer cells transduced with indicated Src constructs. Anchorage-independent growth (**f**) and invasion (**g**) of SW620 cancer cells expressing indicated Src constructs. The histograms show the percentage of colonies in soft agar normalized to the maximal condition set a 100% (colonies) and the percentage of migrating cells in the matrigel matrix normalized to control condition set at 100% (cell invasion). Is shown the mean ± SD; $n = 3$; ns: $p > 0.05$; *$p < 0.05$; **$p < 0.01$; ***$p < 0.001$; Student's t test.

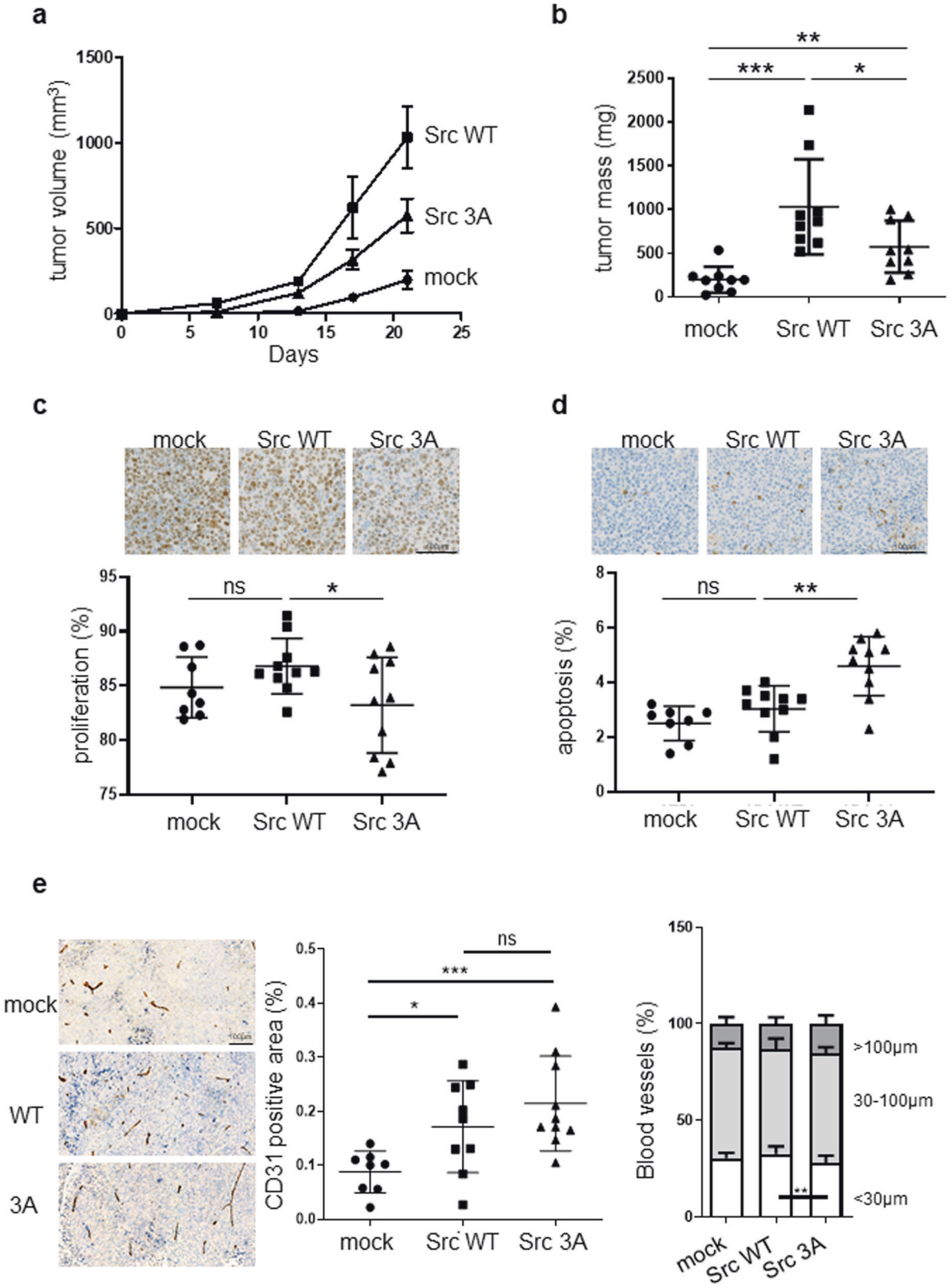

Fig. 3 ULBR inactive mutations affects Src tumor activity in nude mice. a, **b** Time-course of tumor development in nude mice subcutaneously inoculated with SW620 tumor cells that were transduced with control (mock) or indicated Src construct. Analysis of tumor cell proliferation (**c**), apoptosis (**d**) and angiogenesis (**e**) from indicated tumor sections. Representative sections and quantification of immunohistochemical analysis showing tumor cell proliferation (anti-ki67), apoptosis (anti-cleaved Caspase 3) and angiogenesis (anti-CD31; length of blood vessels) in xenograft tumors derived from SW620 cells transduced with indicated Src construct. Is shown the mean ± SEM (**a**) and the mean ± SD (**b**–**e**); $n > 8$ mice per cohort; ns: $p > 0.05$; *$p < 0.05$; **$p < 0.01$; ***$p < 0.001$; Student's t test.

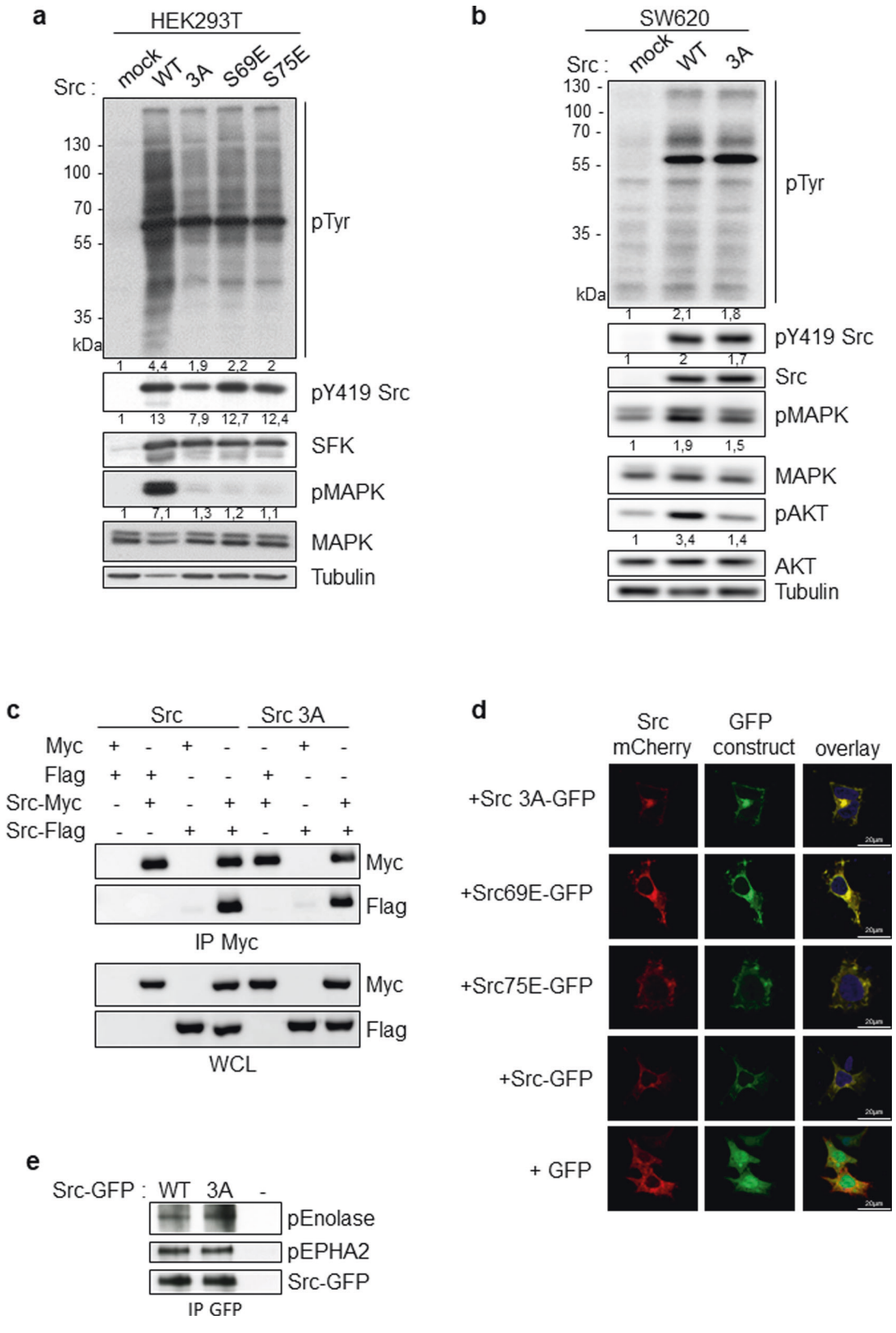

and their co-localization was analyzed by direct fluorescent microscopy. We found an almost strict co-localization between wild-type Src and ULBR-Src mutants, i.e., at perinuclear membranes, endocytic vesicles and membrane cell periphery (Fig. 4d and Supplementary Fig. S3b). A similar subcellular localization pattern was observed from cells expressing wild-type or ULBR-mutant Src-GFP alone (Supplementary Fig. S3c). This results indicate that, although ULBR may modulate the Src topology at the membrane, this region had no impact on Src membrane subcellular localization. Since the cellular Src kinase activity was

Fig. 4 ULBR inactive mutation inhibits MAPK signaling without affecting Src localization and kinase activity. a, **b** ULBR regulates Src-induced protein tyrosine phosphorylation and of p42/44 MAPK activation. Immunoblots and relative band intensity quantification of whole-cell lysates showing cellular protein tyrosine phosphorylation and of p42/44 MAPK activity in HEK293T cells (**a**) and SW620 cells (**b**) transduced with indicated Src constructs ($n = 5$). **c** Src dimerization is not affected by ULBR inactivation. HEK293T cells were transfected with the indicated constructs. Src-Myc proteins were immunoprecipitated (IP) from cell lysates and immunoblotted with the indicated antibodies. Immunoblots of whole-cell lysates were also performed as indicated ($n = 2$). **d** Representative confocal image of direct fluorescence of HEK293T cells co-expressing Src-mCherry and indicated Src-GFP ULBR mutants. The overlay is also shown. **e** In vitro kinase assay of purified Src-GFP and Src3A-GFP that were expressed in HEK293T cells using indicated substrate. The level of immunoprecipitated Src-GFP proteins and tyrosine phosphorylation of indicated substrate is shown ($n = 3$).

affected by ULBR inactivation, we analyzed the impact of ULBR inactivation on Src kinase activity in vitro using enolase, or EPHA2 as substrates [22]. No difference between purified Src-GFP and Src3A-GFP kinase activity was detected in respect to enolase substrate concentration or kinase duration. (Fig. 4e, Supplementary Fig. S4a, b). Similarly, no effect of ULBR inactivation was observed with EPHA2, suggesting that the lack of effect of ULBR mutation in vitro is not substrate specific. Altogether, these data indicate that the observed in vivo effects with ULBR mutants do not depend on Src cell compartmentalization or lipid-induced Src kinase dimerization.

Phospho-proteomic analyses of ULBR-Src signaling in tumor cells

We next characterized ULBR-dependent Src phospho-signaling by proteomic methods. SW620 cancer cells were retrovirally transduced with mock (control), wild-type Src and Src3A constructs. A global tyrosine phospho-proteomic analysis was first performed by phospho-tyrosine peptide immune-purification from trypsin-digested cell lysates followed by label-free mass spectrometry-based quantification [31]. From this analysis, we detected 279 phospho-peptides in control cells with a $\log_2$ fold change (FC) ≥ 1 upon Src (or Src3A) expression (Supplementary Table S1). These Src substrates were essentially composed of signaling proteins, regulators of cell adhesion, trafficking, mRNA maturation, protein synthesis and cell metabolism (Supplementary Table S1), consistent with previous studies [22, 23]. We next examined how these peptides distribute into wild type Src and Src3A expressing samples, using a $\log_2$ FC ≥ 2 threshold. Src- and Src3A-induced protein tyrosine phosphorylation showed very similar profiles (Fig. 5a and Supplementary Table S1), indicating that ULBR has no major impact on Src substrate phosphorylation and/or this region may regulate subtle phosphorylation changes that could not be detected from the label-free MS analysis. We next profiled ULBR signaling by probing a phospho-receptor tyrosine kinase (RTK) antibody array (Fig. 5b and Supplementary Fig. S5). This biochemical survey revealed that Src has a large impact on tyrosine phosphorylation of RTKs (>2-fold increase for 13/49 RTKs), including adhesive receptors DDR2 and EPHs, growth factors receptors EGFR, MET, FGFR3 and AXL an RYK, a co-receptor of the Wnt/beta-catenin signaling (Supplementary Fig. S5). Interestingly, Src-ULBR had a modulatory role on Src-induced RTKs tyrosine phosphorylation, i.e., a positive effect on EGFR, MET, FGFR3, RYK and EPHA2 tyrosine phosphorylation and an inhibitory effect on EPHAB6 tyrosine phosphorylation (Fig. 5b, Supplementary Fig. S5). We also complemented this analysis by probing a phospho-kinase antibody array (Fig. 5c and Supplementary Fig. S5), which revealed that Src expression activates Stats (2, 5 and 6) and SFKs (Fyn, Yes, Lck, Lyn and Hck) signaling proteins. Interestingly, while Src-ULBR was dispensable for most of the probed phospho-signaling activities, it was required for Src-induced Fyn activation (i.e., pTyr420-Fyn level) and activation of the downstream effectors p42/44 MAPKs (i.e., pThr202/pTyr204 level) in these cancer cells (Fig. 5c and Supplementary Fig. S5). We thus concluded that ULBR modulates tyrosine phosphorylation of specific membrane-localized substrates, e.g., RTKs and SFKs.

EPHA2 and Fyn as important mediators of Src-ULBR signaling in tumor cells

Finally, we aimed at validating these results functionally. ULBR inactivation reduced Src-induced p42/44 MAPK and Akt signaling leading to SW620 cell invasion (Figs. 2f and 4b and Supplementary Fig. S2c) and we interrogate the role of two ULBR-dependent Src substrates on this signaling response, i.e., EPHA2 and Fyn. EPHA2 is aberrantly stabilized in colon cancer cells by a Src-dependent mechanism implicating inactivation of the SLAP-UBE4A ubiquitination complex [21]. Moreover, EPHA2 phosphorylation on Tyr594 by Src amplifies Akt signaling, leading to colon cancer cell invasion [21]. Consistent with our proteomic analyses, Src-ULBR regulated EPHA2-Tyr594 phosphorylation (Supplementary Fig S5a). At the functional level, *EPHA2* silencing inhibited Src signaling leading to Akt and p42/44 MAPK activation and cell invasion (Fig. 5d, f, Supplementary Fig. S6a, c, d); however, it had no clear effect on Src3A signaling responses. EPHA2 is thus an important mediator of ULBR-Src signaling in SW620 cells. The fact that Src induces activation of other SFKs, e.g., Fyn, in colon cancer cells raises the idea that Src interacts with other SFKs to induce oncogenic signaling. Consistently, Src expression increased Fyn protein levels (Fig. 5e), likely via a posttranscriptional mechanism because it had no impact on *FYN* transcript level (Supplementary Fig S6b). Functionally, Fyn depletion specifically inhibited Src-induced p42/44 MAPK activation and cell invasion (Fig. 5f and Supplementary Fig. S6d). However, no such inhibitory effect was observed on Src3A signaling placing Fyn as an additional effector of Src-ULBR signaling. The interaction between Src and Fyn signaling was next confirmed by showing a potentiating effect of Fyn on Src-induced p42/44 MAPK activation in HEK293T cells (Supplementary Fig S6e). However, this signaling response was reduced upon Src-ULBR mutation, supporting further a role for Src-UD in Src-Fyn signaling (Supplementary Fig S6e). Overall, our results point to an important role of Src-ULBR in the regulation of membrane substrates phosphorylation, essential for Src tumor signaling.

DISCUSSION

Most eukaryotic proteins have intrinsically disordered regions (IDRs) that challenge the classical structure-function paradigm. Here, we uncover an important role of this molecular property made by Src-UD in cancer development. The biological roles of IDRs contained in SFK have remained unclear, despite strong insight into Src regulation. Previous mutagenesis experiments centered in this region did not reveal any clear oncogenic activity [7], possibly because Src-IDR may contain opposite regulatory sequences that would not be detected with this approach. Consistent with this idea, our mutagenesis analysis guided from our previous NMR data [10, 11, 13, 14, 16] led to specifically inactivate the ULBR, a small region conserved in Src-UD, which revealed its essential role in Src tumor activity. Additionally, our results suggest a phosphorylation-dependent mechanism to regulates this Src tumor activity, although the kinases involved in this process remains to be characterized. This sequence may however not regulate all Src transforming functions, as suggested from Src-induced morphological changes in mouse fibroblasts.

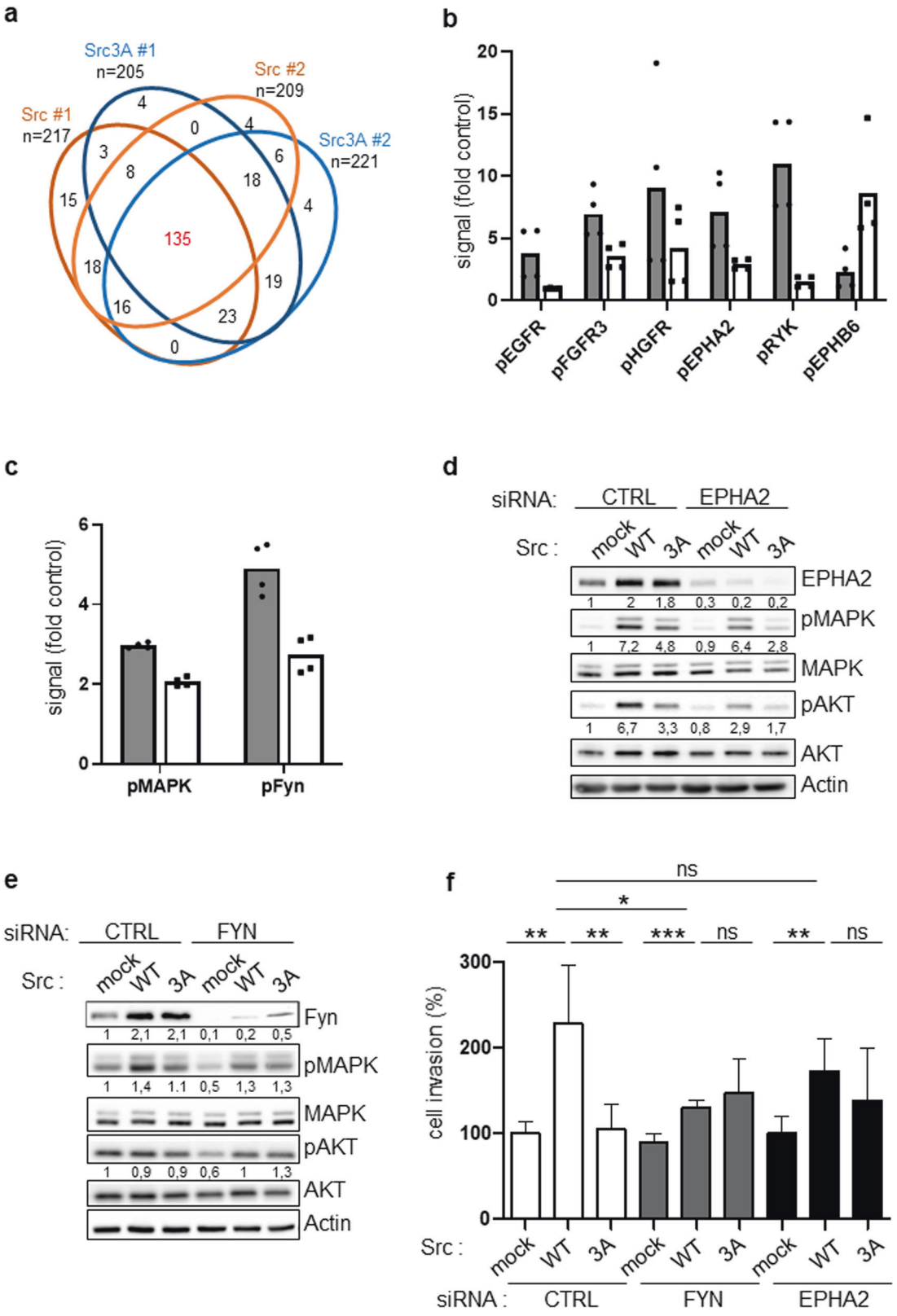

Actually, Src-ULBR may act as a fine-tuning mechanism, which may be exacerbated upon Src overactivation to promote cancer development. This fine-tuning mechanism is supported by previous works on the Src capacity to induce Xenopus oocytes maturation [10], Src regulation of retinal ganglion cell survival or postmitotic neuron function by Ser75 phosphorylation [32, 33] and is consistent with a recent Src optogenetic study [34].

Our study also brings valuable molecular insight into the mechanism of Src regulation by its unstructured region. Previous studies reported that Lck-IDR can mediate protein interaction by

Fig. 5 phospho-proteomic analysis of Src-ULBR signaling in SW620 cancer cells. a A label-free quantitative phospho-proteomic analysis centered on tyrosine phosphorylation. A Veen diagram where quantified phospho-peptides were sorted as differentially phosphorylated from the control condition (mock) (log2FC ≥ 1) in the indicated Src (or Src3A) conditions**. b** A phospho-RTK array approach. **c** A phospho-signaling kinase array approach. Comparison of Src (gray boxes) and Src3A (white boxes) induced tyrosine phosphorylation of RTKs and phosphorylation of signaling kinases. Is shown the phosphorylation level of selected kinases relative to the mock condition (fold control; duplicates from 2 independent experiments). **d–f** Fyn and EPHA2 are important mediators of ULBR-Src signaling in SW620 cancer cells. **d**, **e** Biochemical analysis and relative band intensity quantification of p42/44 MAPK and Akt activity in SW620 expressing or not Src or Src3A mutant as shown and transfected with indicated siRNA ($n = 3$). The level of EPHA2 and Fyn is also shown ($n = 2$). **f** Cell invasion of SW620 expressing or not Src or Src3A mutant and transfected with indicated siRNA. The histograms show the percentage of migrating cells in the matrigel matrix normalized to control condition set at 100% (cell invasion). Is shown the mean ± SD; $n = 4$; ns: $p > 0.05$; *$p < 0.05$; **$p < 0.01$; ***$p < 0.001$; Student's t test.

adopting an organized structure [35]. Whether IDR of other SFKs display similar molecular property is not known, although Src-UD was involved in protein interactions [36]. IDRs adopt multiple conformations that are sensitive to the environment and, through multiple weak interactions in a fuzzy complex, may direct the activity of folded domains of signaling proteins towards different pathways [8]. Our results support such a Src-IDR regulatory mechanism at the plasma membrane since ULBR regulates Src membrane anchoring and phosphorylation of essential membrane-localized substrates of tumor signaling, notably RTKs and SFKs. An unsuspected finding from this work is the Src capacity to activate additional SFKs, such as Fyn, to promote oncogenic signaling. This result suggests the existence of a SFK network involved in cancer development and uncovers a novel layer of Src signaling complexity, which deserves further investigation.

By focusing on ULBR, this work started addressing the biological role of Src-IDR but existing molecular studies uncovered additional regions involved in the fuzzy complex made by SFKs-IDR, which would also contribute to Src regulation. Unraveling the biological role of these regions may bring a more complete view on the complexity of Src regulation by its IDR. Finally, Src has been identified as an attractive target in oncology but Src inhibitors developed for the clinic gave disappointing results in colon cancer, probably because of high toxicity and inefficient Src signaling inhibition [3]. Interestingly, structural analyses of non-catalytic domains of TKs have revealed unique modes of kinase regulation [37], which resulted in the development of allosteric inhibitors with improved anti-tumor activities, as reported for asciminib in chronic myeloid leukemia [38]. We thus propose that targeting the IDR fuzzy complex with small molecules would circumvent some of these issues and therefore may define an attractive strategy to block Src tumor activity in human cancer.

MATERIAL AND METHODS

Antibodies

anti-p42/44 MAPKs (#4695S), anti-p42/44 MAPKs pT202/Y204 (#4370S), anti-p38 MAPK (#9212), anti-p38 MAPK pT180/Y182 (#9211S), anti-AKT (#9272S), anti-AKT pS473 (#4060S), anti-EPHA2 pY594 (#3970S), anti-Src pY419 (#2101L), anti-Stat3 pY705(#9131S) (CST), anti-EPHA2 (#6997S), anti-Stat3 (#9139S), anti-Myc (#2276S) and anti-pTyr clone pY1000 Sepharose bead conjugated (PTM Scan) were from CST, anti-Src specific (2.17) antibody (a gift from Dr S Parsons, University of Virginia, VA, USA), anti-FLAG (M2 antibody, Sigma Aldrich), and anti-GFP (Chromotek), anti-tubulin (gift from N. Morin, CRBM, Montpellier, France), anti-pTyr 4G10 (gift from P. Mangeat, CRBM, Montpellier, France), anti-cst1 (that recognizes Src, Fyn and Yes) was described in [39]. Anti-rabbit IgG-HRP and anti-mouse IgG-HRP (GE Healthcare). Anti-Mib1h (Dako)(KI67), anti-active-caspase3 (AP175; CST), anti-CD31 (Ab28364, Abcam).

Phylogenetic analyses

Nucleic and protein SFK sequences were retrieved from NCBI annotated nr database (http://www.ncbi.nlm.nih.gov). Accessions are listed Supplementary Table S1. Protein sequences were aligned using MAAFT v7.450 [40]. Nucleic sequence alignments were based on protein alignments. Phylogenetic trees were estimated by PhyML [41], using the General Time Reversible (GTR) model with invariant and gamma decorations. Nonsynonymous versus synonymous substitution ratios (ω = dN/dS) were calculated using PAML 4.4 [42]. We compared the "one-ratio" model (a single ω ratio for the entire tree) and the "two-ratio" model (distinct ω values for each of the Src, Fyn and Yes branches) by using the likelihood ratio test.

Plasmids

pMX-pS-CESAR retroviral vector expressing human Src was described in [21]. pMX-Src L63A/F54A/G65A (Src 3A) was described in [11]. The other plasmids were obtained by PCR using the QuickChange Site-Directed Mutagenesis Kit (Stratagene) using specific oligonucleotides as follows: Src S69E, Forward-5′ CGGAGGCTTCAACGCCTCG GACACCGT3′, Reverse-5′ACGGTGTCCGAGGCGT TGAAGCCTCCG3′; Src S75E, Forward-5′GACACCGTCACCGCCCCGCAGAGGG3′, Reverse-5′CCCTCTGCGGGGCG GTGACGGTGTC3′; Src Y530F (Src YF), Forward-5′CGGGCTGGAACTGGGGCTCGGTG G3′, Reverse-5′CCACCGAGCCCCAGTTCC AGCCCG3′. Each of the Y530F counterparts Src L63A/F54A/G65A/Y530F (SrcYF 3A), Src S69E/Y530F (SrcYF S69E); Src S75E/Y530F (SrcYF S75E) were obtained by adding the Y530F mutation using the following oligonucleotides Forward-5′ TCTCGAGCTCAAGCTTAGTACCCTTCACCATGGG TAGCAACAA3′, Reverse-5′ GGCGACCGGTGGATCCGAGCCGGAGCCGAGGTTCT CCCCGG GCTGGTA3′. Src-GFP and Src-mCherry constructs were obtained by insertion of Src sequence (or Src mutants) in pEGFP-N1 and pmCherry N1 respectively including a GluX3 spacer. Src-Flag and Src-Myc constructs were obtained by inserting Src and Src3A sequences in pcDNA3 vectors. pSG5 Fyn construct was described in [19].

Cell cultures, retroviral infections and transfections

Cell lines (NIH3T3, HEK293T and SW620 cells) (ATCC, Rockville, MD) were cultured, transfected and infected as described in [21]. Stable cell lines were obtained by fluorescence-activated cell sorting. For siRNA transfection, 2.10^5 cells were seeded in 6-well plates and transfected with 20 nmol of siRNA and 9 µl of Lipofectamine RNAi Max according to the manufacturer's protocol (ThermoFisher Scientific). A scramble siRNA (siMock) 5′TTCTCCGAACGTGTCACGTTT3′ was used as a negative control (Eurofins). The following siRNAs were used for functional assays: siRNA FYN#1 (Cell Signaling Technology #12473), siRNA FYN#2 5′GGCCCTTTATG ACTATGAATT3′, siRNA EPHA2#1 5′GCAGT ATACGGAGCACTTCTT3′, siRNA EPHA2#2 5′GTATCTTCATTGAGCTCAATT3′ (Eurofins).

Biochemistry

Immunoprecipitation and immunoblotting were performed as described in [21]. Kinase assays were performed as described in [21] using 200 ng of purified EPHA2 recombinant protein (OriGen Technologies) or indicated concentration of purified Enolase (Sigma Aldrich), in the absence or presence of about 50 ng of purified Src-GFP (or Src3A-GFP as indicated) in the presence of 0.1 mM ATP Lithium Salt (Roche Diagnostics) in kinase buffer (20 mM Hepes pH6.5, 10 mM $MnCl_2$, 1 mM DTT) for indicated time at 30 °C. Src-GFP purification was performed by anti-GFP immunoprecipitation from HEK293T cells transfected with Src-GFP (or Src3A-GFP) construct.

RNA extraction and RT-quantitative PCR

mRNA was extracted from cell lines and tissue samples using the RNeasy plus mini kit (Qiagen) according to the manufacturer's instructions. RNA (1 µg) was reverse transcribed with the SuperScript VILO cDNA Synthesis Kit (Invitrogen). Quantitative PCR (qPCR) was performed with the SyBR Green Master Mix in a LightCycler 480 (Roche). Expression levels were normalized with the Tubulin human housekeeping gene. Primers used for qPCR: Tubulin, Forward-5′CCGGACAGTGTGGCAA CCAGATCGG3′,

Reverse-5′TGGCCAAAAGGACCTGAGCG AACGG3′; Fyn, Forward-5′TGACC TCCATCCCCAACTA3′, Reverse-5′TTCCCACCAATCTCCTTCC3′; EPHA2, Forward-5′GGGACCTGATGCAGAACATC3′, Reverse-5′AGTTGGTGCGGAGC CAGT3′.

Cell imaging

HEK293T cells plated on glass coverslips coated with fibronectin were transfected with Src-GFP and Src-mCherry constructs for 24 h and subcellular Src distribution was analyzed after cell fixation (4% paraformaldehyde) by direct fluorescence using confocal microscopy. Src-transformed NIH3T3 cells were plated on glass coverslip coated with fibronectin for 24 h and actin was visualized with Texas red-conjugated phalloidin (1:200 dilution) after cell fixation (4% paraformaldehyde) and permeabilization (0.05% TRITON for 10 min at room temperature).

Soft agar colony formation and cell invasion assay

Colonies formation: 1 000 cells per well were seeded in 12-well plates in 1 ml DMEM containing 10% FCS and 0.33% agar on a layer of 1 ml of the same medium containing 0.7% agar. After 18–21 days, colonies with >50 cells were scored as positive. Cell invasion assay was performed as described in [31] using Fluoroblok invasion chambers (BD Bioscience) in the presence of 100 µl of 1–1.2 mg/ml Matrigel (BD Bioscience).

Phospho-proteomic analyses

Quantitative phosphoproteomics was performed as in [31]. Briefly, SW620 cells were lysed in urea buffer (8 M urea in 200 mM ammonium bicarbonate pH 7.5). Phosphopeptides were purified after tryptic digestion of 20 mg (for cells) or of 35 mg (for mouse tumors) total proteins using the PTMScan® Phospho-Tyrosine Rabbit mAb (P-Tyr-1000) Kit (Cell Signaling Technology), according to manufacturer's protocol. An additional enrichment step using the IMAC-Select Affinity Gel (Sigma Aldrich) was performed to increase the phosphopeptide enrichment. Data are available via ProteomeXchange with identifier PXD030006. Purified phosphopeptides were resuspended in 10% formic acid and two technical replicates for each sample were analyzed. Phospho-kinase arrays: proteome profiler human phospho-kinase array including phosphorylation of 43 kinases (ARY003B) and human phospho-RTK array (ARY001B) kits including 49 RTKs were purchased from R&D Systems. Indicated SW620 cells were lysed, and 300 µg of protein lysates were subjected to western blotting according to the manufacturer's protocol. Signals on membranes were quantified using the Amersham Imager 600 (GE Healthcare) from 2 independent biological replicates.

In vivo experiments and Immunohistochemistry (IHC)

In vivo experiments were performed in compliance with the French guidelines for experimental animal studies (Direction des services vétérinaires, ministère de l'agriculture, agreement B 34–172–27). 2×10^6 SW620 cells (or derivatives) were subcutaneously injected in the flank of 5-week-old female athymic nude mice (Envigo) (8 mice per group). Tumor volumes were measured blinded as the indicated intervals using calipers. After 24 days, tumors were excised, weighed and cryopreserved or processed for subsequent immunohistochemistry analysis as described in [23].

Statistical analysis

All analyses were performed using GraphPad Prism. Data are presented as the mean ± SD, except in Fig. 3a. When distribution was normal (assessed with the Shapiro Wilk test), the two-tailed *t* test was used for between-group comparisons. In the other cases, the Mann–Whitney test was used. Statistical analyses were performed on a minimum of three independent experiments. The statistical significance level is illustrated with *p* values: $*p \le 0.05$, $**p \le 0.01$, $***p \le 0.001$.

REFERENCES

1. Yeatman TJ. A renaissance for SRC. Nat Rev Cancer. 2004;4:470–80.
2. Summy JM, Gallick GE. Src family kinases in tumor progression and metastasis. Cancer Metastasis Rev. 2003;22:337–58.
3. Sirvent A, Mevizou R, Naim D, Lafitte M, Roche S. Src family tyrosine kinases in intestinal homeostasis, regeneration and tumorigenesis. Cancers. 2020;12:2014.
4. Boggon TJ, Eck MJ. Structure and regulation of Src family kinases. Oncogene. 2004;23:7918–27.
5. Arbesú M, Iruela G, Fuentes H, Teixeira JMC, Pons M. Intramolecular fuzzy interactions involving intrinsically disordered domains. Front Mol Biosci. 2018;5:39.
6. Amata I, Maffei M, Pons M. Phosphorylation of unique domains of Src family kinases. Front Genet. 2014;5. https://www.ncbi.nlm.nih.gov/pmc/articles/PMC4075076/.
7. Cross FR, Garber EA, Pellman D, Hanafusa H. A short sequence in the p60src N terminus is required for p60src myristylation and membrane association and for cell transformation. Mol Cell Biol. 1984;4:1834–42.
8. Wright PE, Dyson HJ. Intrinsically disordered proteins in cellular signaling and regulation. Nat Rev Mol Cell Biol. 2015;16:18–29.
9. Fuxreiter M. Fuzziness: linking regulation to protein dynamics. Mol BioSyst. 2011;8:168–77. 1
10. Pérez Y, Maffei M, Igea A, Amata I, Gairí M, Nebreda AR, et al. Lipid binding by the Unique and SH3 domains of c-Src suggests a new regulatory mechanism. Sci Rep. 2013;3:1295.
11. Maffei M, Arbesú M, Le Roux A-L, Amata I, Roche S, Pons M. The SH3 domain acts as a scaffold for the N-terminal intrinsically disordered regions of c-Src. Structure. 2015;23:893–902. 5
12. Spassov DS, Ruiz-Saenz A, Piple A, Moasser MM. A dimerization function in the intrinsically disordered N-terminal region of Src. Cell Rep. 2018;25:449–463.e4. 9
13. Le Roux A-L, Mohammad I-L, Mateos B, Arbesú M, Gairí M, Khan FA, et al. A myristoyl-binding site in the SH3 domain modulates c-Src membrane anchoring. iScience. 2019;12:194–203. 22
14. Arbesú M, Maffei M, Cordeiro TN, Teixeira JMC, Pérez Y, Bernadó P, et al. The unique domain forms a fuzzy intramolecular complex in Src family kinases. Structure. 2017;25:630–640.e4. 4
15. Teixeira JMC, Fuentes H, Bielskutė S, Gairi M, Żerko S, Koźmiński W, et al. The two isoforms of lyn display different intramolecular fuzzy complexes with the SH3 domain. Molecules. 2018;23:2731.
16. Pérez Y, Gairí M, Pons M, Bernadó P. Structural characterization of the natively unfolded N-terminal domain of human c-Src kinase: insights into the role of phosphorylation of the unique domain. J Mol Biol. 2009;391:136–48. 7
17. Amata I, Maffei M, Igea A, Gay M, Vilaseca M, Nebreda AR, et al. Multi-phosphorylation of the intrinsically disordered unique domain of c-Src studied by in-cell and real-time NMR spectroscopy. ChemBioChem. 2013;14:1820–7.
18. Yokouchi M, Kondo T, Sanjay A, Houghton A, Yoshimura A, Komiya S, et al. Src-catalyzed phosphorylation of c-Cbl leads to the interdependent ubiquitination of both proteins. J Biol Chem. 2001;276:35185–93. 14
19. Manes G, Bello P, Roche S. Slap negatively regulates Src mitogenic function but does not revert Src-induced cell morphology changes. Mol Cell Biol. 2000;20:3396–406.
20. Sirvent A, Bénistant C, Pannequin J, Veracini L, Simon V, Bourgaux J-F, et al. Src family tyrosine kinases-driven colon cancer cell invasion is induced by Csk membrane delocalization. Oncogene. 2010;29:1303–15. 4
21. Naudin C, Sirvent A, Leroy C, Larive R, Simon V, Pannequin J, et al. SLAP displays tumour suppressor functions in colorectal cancer via destabilization of the SRC substrate EPHA2. Nat Commun. 2014;5:3159.
22. Leroy C, Fialin C, Sirvent A, Simon V, Urbach S, Poncet J, et al. Quantitative phosphoproteomics reveals a cluster of tyrosine kinases that mediates SRC invasive activity in advanced colon carcinoma cells. Cancer Res. 2009;69:2279–86. 15
23. Sirvent A, Vigy O, Orsetti B, Urbach S, Roche S. Analysis of SRC oncogenic signaling in colorectal cancer by stable isotope labeling with heavy amino acids in mouse xenografts. Mol Cell Proteom. 2012;11:1937–50.
24. Lecointre C, Simon V, Kerneur C, Allemand F, Fournet A, Montarras I, et al. Dimerization of the pragmin pseudo-kinase regulates protein tyrosine phosphorylation. Structure. 2018;26:545–554.e4. 3
25. Sirvent A, Benistant C, Roche S. Oncogenic signaling by tyrosine kinases of the SRC family in advanced colorectal cancer. Am J Cancer Res. 2012;2:357–71.
26. Turkson J, Bowman T, Adnane J, Zhang Y, Djeu JY, Sekharam M, et al. Requirement for Ras/Rac1-mediated p38 and c-Jun N-terminal kinase signaling in Stat3 transcriptional activity induced by the Src oncoprotein. Mol Cell Biol. 1999;19:7519–28.
27. Bowman T, Broome MA, Sinibaldi D, Wharton W, Pledger WJ, Sedivy JM, et al. Stat3-mediated Myc expression is required for Src transformation and PDGF-induced mitogenesis. Proc Natl Acad Sci USA. 2001;98:7319–24. 19
28. Le Roux A-L, Busquets MA, Sagués F, Pons M. Kinetics characterization of c-Src binding to lipid membranes: Switching from labile to persistent binding. Colloids Surf B Biointerfaces. 2016;138:17–25. 1
29. Veracini L, Franco M, Boureux A, Simon V, Roche S, Benistant C. Two distinct pools of Src family tyrosine kinases regulate PDGF-induced DNA synthesis and actin dorsal ruffles. J Cell Sci. 2006;119:2921–34. 15
30. Le Roux A-L, Castro B, Garbacik ET, Garcia Parajo MF, Pons M. Single molecule fluorescence reveals dimerization of myristoylated Src N-terminal region on supported lipid bilayers. ChemistrySelect. 2016;1:642–7. 1
31. Jeitany M, Leroy C, Tosti P, Lafitte M, Le Guet J, Simon V, et al. Inhibition of DDR1-BCR signalling by nilotinib as a new therapeutic strategy for metastatic colorectal cancer. EMBO Mol Med. 2018;10:e7918.

32. Kashiwagi K, Ito S, Maeda S, Kato G. A Ser75-to-Asp phospho-mimicking mutation in Src accelerates ageing-related loss of retinal ganglion cells in mice. Sci Rep. 2017;7:16779. 1
33. Kato G. Nonphosphorylatable Src Ser75 mutation increases ethanol preference and consumption in mice. eNeuro. 2019;6:e0418–18.2019 1–1.
34. Kerjouan A, Boyault C, Oddou C, Hiriart-Bryant E, Grichine A, Kraut A, et al. Control of SRC molecular dynamics encodes distinct cytoskeletal responses by specifying signaling pathway usage. J Cell Sci. 2021;134:jcs254599.
35. Kim PW, Sun Z-YJ, Blacklow SC, Wagner G, Eck MJ. A zinc clasp structure tethers Lck to T cell coreceptors CD4 and CD8. Science. 2003;301:1725–8. 19
36. Yu XM, Askalan R, Keil GJ, Salter MW. NMDA channel regulation by channel-associated protein tyrosine kinase Src. Science. 1997;275:674–8. 31
37. Nagar B, Hantschel O, Young MA, Scheffzek K, Veach D, Bornmann W, et al. Structural basis for the autoinhibition of c-Abl tyrosine kinase. Cell. 2003;112:859–71. 21
38. Eide CA, Zabriskie MS, Savage Stevens SL, Antelope O, Vellore NA, Than H, et al. Combining the allosteric inhibitor asciminib with ponatinib suppresses emergence of and restores efficacy against highly resistant BCR-ABL1 mutants. Cancer Cell. 2019;36:431–443.e5. 14
39. Roche S, Fumagalli S, Courtneidge SA. Requirement for Src family protein tyrosine kinases in G2 for fibroblast cell division. Science. 1995;269:1567–9. 15
40. Katoh K, Standley DM. MAFFT multiple sequence alignment software version 7: improvements in performance and usability. Mol Biol Evol. 2013;30:772–80.
41. Guindon S, Gascuel O. A simple, fast, and accurate algorithm to estimate large phylogenies by maximum likelihood. Syst Biol. 2003;52:696–704.
42. Yang Z. PAML 4: phylogenetic analysis by maximum likelihood. Mol Biol Evol. 2007;24:1586–91.

ACKNOWLEDGEMENTS

We thank the Montpellier RIO Imaging and RHEM platforms for imaging and immunohistochemistry analyses, and the Proteomic Core Platform of EPFL for proteomic analyses. This work was supported by Fundació Marató de TV3, Spanish Ministry of Science and Innovation (project PID2019-104914RB-I00), La Ligue Nationale Contre le Cancer (LNCC), Montpellier SIRIC Grant «INCa-DGOS-Inserm 6045», ANR, CNRS, and the University of Montpellier. RHEM facility supported by SIRIC Montpellier Cancer Grant INCa_Inserm_DGOS_12553, the european regional development foundation and the occitanian region (FEDER-FSE 2014-2020 Languedoc Roussillon), IBiSA and Ligue contre le cancer for processing our animal tissues and histology technics. ML is supported by the Fondation pour la Recherche Médicale (FRM) and the Fondation de France. SR is an INSERM investigator.

AUTHOR CONTRIBUTIONS

All authors contributed extensively to the work presented in this paper. Experimental analysis and Data acquisition: EA, ML, MB, VS, BR, EF, YB, MM, FA, RH, JP and AS. Bioinformatic analyses: PF, MA and RH. Writing of the paper: SR and MP. Project supervision: SR.

COMPETING INTERESTS

The authors declare no competing interests.

ADDITIONAL INFORMATION

Supplementary information The online version contains supplementary material available at https://doi.org/10.1038/s41388-021-02092-x.

Correspondence and requests for materials should be addressed to Miquel Pons or Serge Roche.

Reprints and permission information is available at http://www.nature.com/reprints

Publisher's note Springer Nature remains neutral with regard to jurisdictional claims in published maps and institutional affiliations.